Electrochemical fabrication and interfacial charge-transfer process of Ni/GaN(0001) electrodes

Journal:	*Physical Chemistry Chemical Physics*
Manuscript ID	CP-ART-11-2015-007378.R1
Article Type:	Paper
Date Submitted by the Author:	20-Jan-2016

Complete List of Authors:	Qin, Shuang-jiao; Suzhou Institute of Nano-tech and Nano-bionics, Chinese Academy of Sciences, Peng, Fei; Suzhou Institute of Nano-tech and Nano-bionics, Chinese Academy of Sciences, Chen, Xue-Qing; Suzhou Institute of Nano-tech and Nano-bionics, Chinese Academy of Sciences, Pan, Ge-Bo; Suzhou Institute of Nano-tech and Nano-bionics, Chinese Academy of Sciences,

Journal Name

ARTICLE

Electrochemical fabrication and interfacial charge-transfer process of Ni/GaN(0001) electrodes

Received 00th January 20xx,
Accepted 00th January 20xx

DOI: 10.1039/x0xx00000x

www.rsc.org/

Shuang-Jiao Qin,[a, b] Fei Peng,[a] Xue-Qing Chen,[a] Ge-Bo Pan[a,*]

Abstract: The electrodeposition of Ni on single-crystalline n-GaN(0001) film from acetate solution was investigated by scanning electron microscopy, X-ray diffraction, energy dispersive X-ray analysis, atomic force microscopy, and electrochemical techniques. The as-deposited Ni/n-GaN(0001) had a flatband potential of U_{fb} = -1.0 V vs. Ag/AgCl, which was much lower than that of bare GaN(0001). That is, a more feasible charge-transfer process occurred at the Ni/n-Ga(0001) interface. On the basis of Tafel plot, an exchange current density of ~ 1.66×10^{-4} mA cm^{-2} was calculated. The nuclei density increased when the applied potential was varied from -0.9 V to -1.2 V and, eventually the whole substrate was covered. In addition, the current transient measurements revealed that the Ni deposition process followed the instantaneous nucleation in 5 mM $Ni(CH_3COO)_2$+ 0.5 M H_3BO_3.

Introduction

Semiconductor electrodes possessing unique physical and chemical properties were distinct from conventional metal ones. Their electronic properties are strongly dependent on the growth conditions.[1-7] These included doping, band structure, charge-transfer, and weak metal/substrate interaction, which resulted in complicated thermodynamics and kinetics in electrochemical process.[8-10] A deep understanding of interfacial charge-transfer process was thus highly desired for their electrochemical and photocatalytic applications.[11-13] Among various semiconductor electrodes (e.g., titanium dioxide, indium tin oxide, and tungsten oxide), gallium nitride (GaN)-based materials had recently attracted a surge of interest.[14,15] They displayed excellent chemical and thermal stability, large potential window for water electrolysis, and low background current.[16,17] Moreover, the midgap states of n-GaN were found to play a key role in mediating the interfacial charge-transfer in an electrolyte.[18]

The chemical control of interfacial charge-transfer kinetics could be achieved by either deposition of thin metal overlayers onto electrode or addition of suitable redox agents to electrolyte. Compared with other metal ones, the nickel layers had attracted great attention and were widely used in protection and decoration industries, due to their excellent chemical stability and mechanical properties.[19-22] Besides, they were used in fabricating micro-mechanical devices, magnetic sensors, and magnetic recording heads.[24-26] Thus, various methods were developed to deposit Ni layers, and the electrodeposition method was of particular interest due to its simplicity and versatility. Recent work demonstrated that the electrodeposited Ni film could be an alternative supporting substrate of GaN-based light-emitting diodes to sapphire.[23] However, the growth mechanism of Ni on GaN was still unclear yet.

Herein, we reported on a detailed study of the electrodeposition of Ni on single-crystal n-GaN(0001) in 5 mM $Ni(CH_3COO)_2$ + 0.5 M H_3BO_3. The interfacial charge-transfer process of Ni/n-GaN was explored for the first time by cyclic voltammetry (CV), impedance-potential, open circuit potential (OCP) in PBS buffer solution with and without UV light illumination. The electrochemical reduction of Ni from acetate solution was investigated by basal electrochemical techniques, including cyclic voltammetry (CV), chronoamperometry (CA), and Tafel measurement. The structure and morphology of the Ni deposits were characterized by scanning electron microscopy (SEM), X-ray diffraction (XRD), atomic force microscopy (AFM), and energy dispersive X-ray analysis (EDAX).

Results and Discussion

Without UV light illumination, the apparent current onset of n-GaN is observed at -1.0 V vs. Ag/AgCl and a maximum cathodic current density of -1.2×10^{-1} mA cm^{-2} is recorded at a cathodic polarization of -1.5 V vs. Ag/AgCl (Fig. 1a). In contrast, the CV of Ni/n-GaN reveals an earlier and much more abrupt onset with strongly enhanced hydrogen evolution. This leads to an increase in the cathodic current to -3.6 mA cm^{-2} at the same

[a] Suzhou Institute of Nano-tech and Nano-bionics, Chinese Academy of Sciences, 215123 Suzhou, P. R. China.
[b] Department of Chemistry, College of Sciences, Shanghai University, 99 Shangda Road, 200444 Shanghai, P. R. China
† E-mail address: gbpan2008@sinano.ac.cn, Fax: +86 512 62872663

cathodic polarization. The shift of the cathodic onset potential is investigated by impedance spectroscopy. For n-GaN surfaces, a flatband potential of U_{fb} = -1.23 V vs. Ag/AgCl is obtained (Fig. 1c), in accordance with literature values.[27] For Ni/n-GaN, the flat

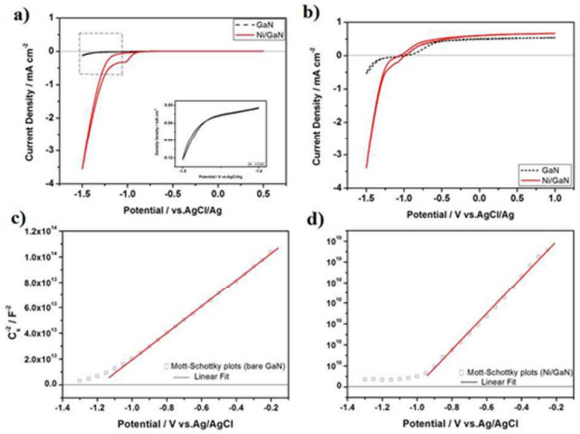

Fig. 1 Cyclic voltammograms of n-GaN and Ni/n-GaN in the dark (a) and under illumination with UV light (b). (c) and (d) Mott-Schottky plots of n-GaN and Ni/n-GaN in PBS.

band potential decreases to -1.0 V vs. Ag/AgCl (in Fig. 1d), indicating a slightly smaller average band-bending in this case. Meanwhile, under the above-mentioned bandgap illumination, there is a bigger difference between bare n-GaN and Ni/n-GaN (Fig, 1b). The shift in the current onset potential is -30 mV between Ni/n-GaN and n-GaN.

Fig. 2a and 2b shows OCP measurements of the Ni/n-GaN structures and n-GaN in PBS. For n-GaN, an initial surface photovoltage (SPV) of 0.97 V is measured upon above-bandgap illumination. After switching off the light, the SPV remains stable for several illumination cycles, which indicates that bare n-GaN is much stabilized. In contrast, n-GaN with deposited Ni exhibits an initial SPV of 0.48 V and after switching off the light,

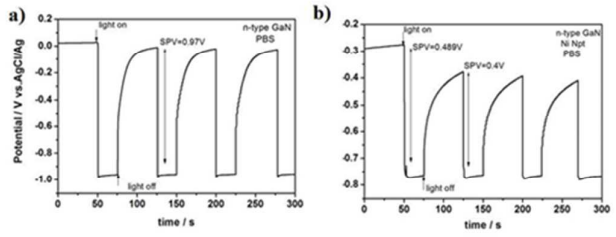

Fig. 2 (a) Open-circuit potential of n-GaN over several illumination cycles in PBS, (b) and with deposited Ni.

long transients are recorded, thus indicating the charging of strong surface state in PBS under UV light illumination. In addition, the initial SPV decreases to 0.4 V in subsequent illumination cycles (Fig. 2b). The difference of initial SPV between n-GaN and Ni/n-GaN is in line with the difference in surface band-bending as obtained by impedance spectroscopy. After switching off the light, the transient response is significantly slower than that for n-GaN surfaces, thus confirming an enhanced charge-transfer rate for these interfaces. CV is widely investigated to study electrochemical processes that occur during a potential sweep. Fig. 3a shows typical CVs of Ni on n-GaN electrodes in $Ni(CH_3COO)_2$ + 0.5 M H_3BO_3 at a scan rate of 10 mV/s. Each voltammogram started from -0.35 V. The cathodic current starts to increase when the potential reaches -0.75 V, indicating the beginning of deposition. The Ni deposition may contain two paths, the first path:

$$Ni^{2+} + 2e^- \rightarrow Ni$$

the second path may include the intermediate products, $NiOH^+$, so the reaction formula is:

$$Ni_2^+ + H_2O \leftrightarrow NiOH^+_{(aq)} + H^+,$$

$$NiOH^+_{(aq)} \leftrightarrow NiOH^+_{ads},$$

$$NiOH^+_{(ads)} + e^- \rightarrow NiOH,$$

$$NiOH + H^+ + e^- \rightarrow Ni + H_2O$$

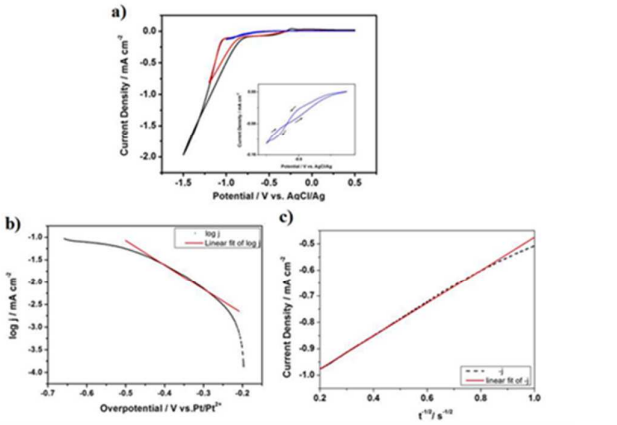

Fig. 3 (a) Cyclic voltammograms of n-GaN(0001). The scan rate is 20 mV s^{-1}, the inset is amplifying figure. (b) Tafel plot. The scan rate is 5 mV s^{-1}. (c) Cottrell plot for the determination of the diffusion coefficient of Ni^{2+} species.

The cathodic current decreases sharply at about -1.0 V vs. Ag/AgCl, which is caused by the hydrogen evolution. A typical Tafel plot corresponding to the Ni electrodeposition onto n-GaN from 5 mM $Ni(CH_3COO)_2$ + 0.5 M H_3BO_3 is shown in Fig. 3b. The plot indicates that a small portion of the curve exhibits a linear relationship in the plot of log j versus overpotential as the mass transfer process quickly becomes the limited-step. The cathodic exchange current density has been estimated ~ 1.66×10^{-4} mA cm^{-2}. And diffusion of electroactive species in solution can be quantitatively described from the diffusion coefficient (D_j, cm^2 s^{-1}), which was evaluated by the Cottrell equation.

$$|j| = nFD_j^{1/2}C_0^*\pi^{-1/2}t^{-1/2} = mt^{-1/2} + b$$

j (A) is the cathodic current density, n is the number of electrons exchanged, D_j represents the diffusion coefficient, and is the concentration of the [Ni^{2+}]. Before the occurrence of the limiting current, by plotting |j| = f ($t^{-1/2}$), a linear graph would be obtained until the growing diffusion layer has reached its maximum width.

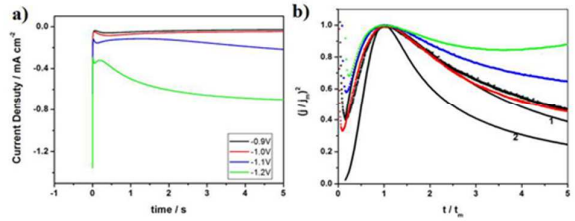

Fig. 4 (a) Potentiostatic current transients of Ni/n-GaN electrodes. (b) Corresponding non-dimensional plots of $(j / j_m)^2$ vs. (t / t_m), theoretical normalized curves for instantaneous (curve 1) and progressive (curve 2) nucleation. Deposition potential range is from -0.9 V to -1.2 V.

The linear part of the experimental Cottrell plot can be seen in Fig. 3c as well as the corresponding data fit. A low diffusion coefficient of $D_j = 1.32\times10^{-6}$ cm^2 s^{-1} is found for Ni^{2+} species.

In order to study and describe the deposition process of Ni on GaN electrode, the potentiostatic transients are recorded at different concentration of $Ni(CH_3COO)_2$ and can be analyzed on the basis of the Scharifker and Hills (SH) model, which is limited by diffusion. In the SH theory, there are two models, including progressive and instantaneous nucleation. In the progressive nucleation, the number of nuclei increases with reaction time, while all nuclei form on the active surface sites of electrode in instantaneously.

The Eqs. 1 and 2 represents the three-dimensional (3D) progressive nucleation and instantaneous nucleation, respectively.

$$\left(\frac{j}{j_m}\right)^2 = \frac{1.2254}{t/t_m}\left\{1-\exp[-2.3367(\frac{t}{t_m})^2]\right\}^2 \quad (1)$$

for the progressive case and:

$$\left(\frac{j}{j_m}\right)^2 = \frac{1.9542}{t/t_m}\left\{1-\exp[-1.2564(\frac{t}{t_m})]\right\}^2 \quad (2)$$

for the instantaneous case.

Fig. 4b shows the non-dimensional plots of $(j / j_m)^2$ versus (t / t_m), transforming from the curves in Fig. 4a, as comparing to the theoretical curves for instantaneous and progressive nucleation. From the results in Fig. 4b, it is found that Ni is forming following the instantaneous nucleation mode at -0.9 V and -1.0 V, while the experimental data depart from the instantaneous curve at -1.1 V and -1.2 V. The nucleation mode cannot be confirmed because only a few data points are presented when the current achieved maximum initially.

Fig. 5a – 5d shows a family of SEM images of Ni deposited on n-GaN substrates in 5 mM $Ni(CH_3COO)_2$ and 0.5 M H_3BO_3 solution. The applied potential is varied from -0.9 V, -1.0 V, -1.1 V to -1.2 V. It can be seen that Ni nuclei are formed on GaN electrode and following with a 3D island growth (Volmer–Weber) mechanism because of the weak interaction between n-GaN and Ni. The nuclei density increases when the applied

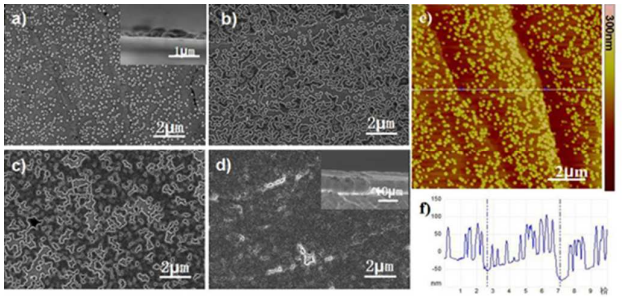

Fig. 5 (a) - (d) are the SEM of Ni electrodeposition on n-GaN(0001) and the applied potential is (a) -0.9 V (b) -1.0 V (c) -1.1 V (d) -1.2 V. The inset is the cross section of Ni/n-GaN. Deposition time is 15 min. (e) AFM micrograph (10×10 μm^2) of Ni/GaN surface. (f) Cross-section profile of 2D image.

potential is varied from -0.9 V to -1.2 V and cover the substrate gradually, however the number of Ni nanoparticles at -1.2 V is similar to the -0.9 V. It is indicated that the active sites of substrate surface are fully occupied by the Ni nanoparticles. The inset is the cross-section of Ni/n-GaN and the inset of Fig. 5a and Fig. 5d are the interaction Ni and n-GaN. Fig. 5e shows the AFM micrograph (10×10 μm2) of Ni/n-GaN surface, the applied potential is -0.9 V and the deposition time is 15 min. In addition,

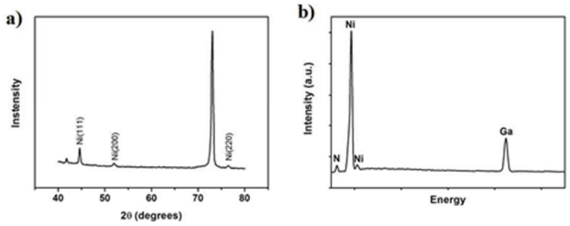

Fig.6 (a) XRD pattern of Ni electrodeposition on n-GaN electrode and (b) EDAX spectrum. The applied potential is -1.2 V and deposition time is 15 min.

the distribution and the size of particles are relatively uniform. Fig. 5f is the cross-section profile of 2D image of Fig. 5e. It is found that the height of Ni nanoparticles is about 60 nm and the height of the particles is similar in the same direction. Fig. 6a and 6b show the XRD and EDAX spectra of Ni nanoparticle deposited on n-GaN. The applied voltage was -1.2 V, and the deposition time is 15 min. The XRD pattern (Fig. 6a) reveals three characteristic peaks around 44.5, 51.8, 76.4°, which are attributed the Ni diffraction peaks of the (111), (200) and (220)

planes (JCPDS Card Number 87-0712), respectively. In addition, the other peaks in the XRD pattern can be indexed to the lattice planes of sapphire and Si doped GaN. Besides the peaks of nitrogen and gallium elements, only the peak of Ni element is found in the EDAX spectrum (Fig. 6b). This indicates that the deposits on the GaN electrode are made of pure elementary substance Ni.

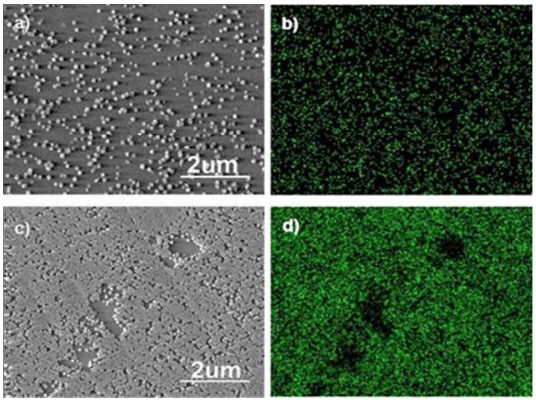

Fig. 7 (a) and (c) typical SEM images of Ni nanoparticles. (b) and (d) corresponding EDS maps of (a) and (c). The applied potentials for the growth of Ni nanoparticles were -0.9 V for (a)-(b) and -1.1 V for (c) and (d).

Fig. 7 shows the EDS maps of Ni distribution on the surface for different experimental conditions. It is noted that the diffraction radius of EDS maps used in the present study is about 1 μm and the spacing between neighboring Ni nanoparticles is less than 1 μm. This indicates that there is no Ni distribution on the blank area of GaN in Fig. 7a and 7b.

Experimental

Single-crystal n–GaN(0001) films were grown on sapphire(0001) by a hydride vapor phase epitaxy, which is comparable to the metal-organic vapor phase epitaxy and molecular beam epitaxy.[4,5] The GaN layer was 5 μm thick, Si-doped, and with a carrier concentration of 4×10^{18} cm^{-3}. Nickel acetate ($Ni(CH_3COO)_2$), boric acid (H_3BO_3), phosphate buffered saline (PBS), ethanol, and acetone were of analytical grade and purchased from Sinopharm Chemical Reagent Co., Ltd. All solutions were prepared by using Milli-Q water (>18 MΩ). All the reagents were used as received.

The working electrode of GaN was ultrasonicated in acetone, ethanol, and DI water for 15 min, rinsed in DI water. An Ohmic
contact was formed on the corner of wafer by applying indium point. The Pt wires (1 mm in diameter) were used as counter electrodes. The electrolytes were prepared by dissolving $Ni(CH_3COO)_2$ into 50 mL mixture solution of 0.5 M H_3BO_3, and the pH and concentration of PBS were 7.0 and 0.2 M.

The electrochemical experiments were undertaken at room temperature with a CHI 660D potentiostat/galvanostat (Shanghai ChenHua Co., Ltd.) and used a standard three-electrode cell arrangement (Scheme 1). All the potentials were reported with respect to the Ag/AgCl reference electrode. The distance between working and counter electrodes is 1 cm.

The morphology of Ni deposits was investigated by means of scanning electron microscopy (Hitachi S4800). The X-ray diffraction (XRD) patterns were recorded on a Bruker D8 Advance power X-ray diffractometer at a scanning rate of 0.04° s-1 in the 2θ range 40 to 80° using Cu-Ka radiation (λ = 1.5406 Å).

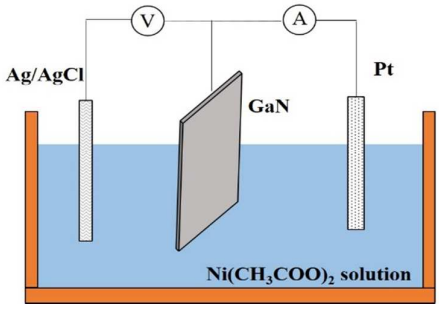

Scheme 1. Schematic drawing of a standard three-electrode cell arrangement.

The energy dispersive X-ray analysis (EDAX) and mapping (EDS) were performed on a Quanta 400 FEG SEM at 20 KV. Atomic force microscopy (AFM) was carried out with Dimension 3100.

Conclusion

The electrodeposition of Ni on single-crystal n-GaN(0001) from acetate solution is investigated by SEM, XRD, EDAX, AFM, and electrochemical techniques (e.g., CV, CA, EIS, and Tafel measurements). On the basis of Tafel plot, an exchange current density of ~ 1.66×10^{-4} mA cm^{-2} is calculated. For bare n-GaN surfaces, the flatband potential is -1.23 V vs. Ag/AgCl, which is in accordance with the literature reported, and the flatband potential of Ni/n-GaN is -1.0 V vs. Ag/AgCl. The nuclei density increases when the applied potential is varied from -0.9 V to -1.2 V and cover the substrate gradually, however the number of Ni nanoparticles at -1.2 V is similar to the -0.9 V. It is indicated that the active sites of substrate surface are fully occupied by the Ni nanoparticles.

Acknowledgements

This work is supported by the National Natural Science Foundation of China (No. 21273272), Key Research Program of Jiangsu Province (No. BE2015073), and the Chinese Academy of Sciences.

References

1 Y. S. Cho, H. Hardtdegen, N. Kaluza, N. Thillosen, R. Steins, Z. Sofer, and H. Lüth, Phys. Status Solidi C, 2006, **3**, 1408.
2 R. Calarco, M. Marso, T. Richter, A. Aykanat, R. Meijers, A. v.d. Hart, T. Stoica, and H. Lüth, Nano. Lett., 2005, **5**, 981.
3 W. Bronger, H. Hardtdegen, M. Kanert, P. Müller, D. Schmitz, Z. Anorg. Chem., 1996, **622**, 313.

4 V. Frese, G.K. Regel, H. Hardtdegen, A. Brauers, P. Balk, M. Hostalek, M. Lokai, L. Pohl, A. Miklis, and K. Werner, J. Electron Mater., 1990, **19**, 305.
5 H. Hardtdegen, M. Pristovsek, H. Menhal, J.-T. Zettler, W. Richter, D. Schmitz, J. Cryst. Growth, 1998, **195**, 211.
6 H. Hardtdegen, M. Hollfelder, R. Meyer, R. Carius, H. Münder, S. Frohnhoff, D. Szynka, H. Lüth, J. Cryst. Growth, 1992, **124,** 420.
7 Th. Schäpers, A. Kaluza, K. Neurohr, J. Malindretos, G. Crecelius, A. van der Hart, H. Hardtdegen, and H. Lüth, Appl. Phys. Lett., 1997, **71**, 3575.
8 P. Allongue, E. Souteyrand, J. Electroanal. Chem., 1990, **286,** 217.
9 P. Allongue, E. Souteyrand, J. Electroanal. Chem., 1993, **362,** 79.
10 P. Allongue, E. Souteyrand, L. Allemand, J. Electroanal. Chem., 1993, **362,** 89.
11 N. S. Lewis, J. Electroanal. Chem., 2001, **508,** 1.
12 N. S. Lewis, Inorg. Chem., 2005, **44,** 6900.
13 S. Schäfer, S. A. Wyrzgol, J. A. Lercher, M. Stutzmann, and I. D.Sharp, ChemCatChem, 2013, **5,** 3224.
14 S. J. Pearton, F. Ren, A. P. Zhang, K. P. Lee, Mater. Sci. Eng., 2000, **30,** 55.
15 T. Someya, R. Werner, A. Forchel, M. Catalano, R. Cingolani, and Y. Arakawa, Science, 1999, **285,** 1905.
16 Y. Li, Y. Zhao, G.-B. Pan, Z.-H. Liu, G.-L. Xu, K. Xu, Electrochim. Acta, 2013, **114,** 352.
17 R. Morita, T. Narumi, N. Kobayashi, Jpn. J. Appl. Phys. Part 1, 2006, **45,** 2525.
18 S. Schäfer, A. H. R. Koch, A. Cavillini, M. Stutzmann, I. D. Sharp, J. Phys. Chem. C, 2012, **116,** 22281.
19 Y. M. Frauq Marikar, K. I. Vasu, Electrodepos. Surf. Treat., 1974, **2,** 281.
20 Y. M. Frauq Marikar, K. I. Vasu, Electrodepos. Surf. Treat., 1974, **2,** 295.
21 J. C. Puippe, N. Ibl, Plat. Surf. Finish., 1980, **67,** 68.
22 L. M. Jiang, J. Peng, Y. G. Liao, Y. C. Zhou, J. Liang, H. X. Hao, C. Lu, Thin Solid Films, 2011, **519,** 3249.
23 S. Kim, J. Electron. Soc., 2012, **159,** 196.
24 B. Lochel, A. Maciossek, H. Quenser, D. K. Wagner, Sensors Actuators, 1995, **46,**98.
25 E. Gomes, E. Valles, J. Appl. Electrochem., 1999, **29,** 805.
26 B. Lochel, A. Maciossek, J. Electrochem. Soc., 1996, **143,** 3343.
27 I. M. Huygens, K. Strubbe, W. P. Gomes, J. Electrochem. Soc., 2000, **147,** 1797.